

# Cable-Driven Parallel Robot (CDPR) for Panelized Envelope Retrofits: Feasible Workspace Analysis

Yifang Liu, Rui Zhang, Nolan W. Hayes, Diana Hun, and Bryan P. Maldonado

Buildings and Transportation Science Division, Oak Ridge National Laboratory, United States of America \*

liuy5@ornl.gov zhangr2@ornl.gov hayesnw@ornl.gov hunde@ornl.gov maldonadobp@ornl.gov

## Abstract -

Recent decades have seen remarkable progress in the field of robotic-assisted construction. Cable-driven parallel robots (CDPRs) emerge as promising tools for automating construction processes, due to their advantageous features such as scalability, reconfigurability, compact design, and high payload-to-weight ratio. This paper uses a simple static model to determine the feasibility of a CDPR for overclad panel installation in building envelope retrofits. Given that the building facade needs to be a subset of the CDPR's wrench-feasible workspace, we focus on the sensitivity of the workspace concerning various cable arrangements and CDPR frame sizes (e.g., height and width extensions). Our analysis indicates that no cable arrangement satisfies the requirement of complete facade coverage and avoids cable-to-panel collisions. Thus, frame extension is needed to enhance coverage. However, in densely populated areas where width extension is limited by space constraints, height extension alone is insufficient to guarantee full facade coverage. This paper pioneers the investigation of CDPRs for panelized envelope retrofits, showcasing their advantages and limitations and paving the way for further research and development.

## Keywords -

CDPR, construction robotics, panelized envelope, envelope retrofits

## 1 Introduction

Buildings account for more than 35% of the total carbon dioxide emissions in the United States [1]. About 52% of the existing residential buildings were built before the implementation of the 1980 energy codes [2]. Consequently, these buildings are more likely to have inadequate thermal insulation and air barriers, or none altogether [3]. The absence of adequate insulation and airtightness in these structures leads to high energy losses through the building envelope that account for 70% of carbon emissions

\*Notice: This manuscript has been authored by UT-Battelle, LLC, under contract DE-AC05-00OR22725 with the US Department of Energy (DOE). The US government retains and the publisher, by accepting the article for publication, acknowledges that the US government retains a nonexclusive, paid-up, irrevocable, worldwide license to publish or reproduce the published form of this manuscript, or allow others to do so, for US government purposes. DOE will provide public access to these results of federally sponsored research in accordance with the DOE Public Access Plan (<https://www.energy.gov/doe-public-access-plan>).



Figure 1. Conceptual view of a cable-driven parallel robot for retrofitting a residential building using overclad panels in a densely populated urban area.

generated locally by households [4]. Therefore, bringing these outdated structures in line with current energy codes can reduce energy usage and greenhouse gas emissions in the building sector. Overclad panel envelope retrofits using prefabricated panels effectively minimize waste and improve energy efficiency [5]. Traditional approaches for installing overclad panels in multi-story buildings typically involve panels being carried by laborers or hoisted with a crane and placed at their final location by hand [6]. These practices incur installation errors, safety concerns for construction workers, low efficiency, and complications in densely populated urban areas due to limited space and disruptions to adjacent structures and pedestrians. Robotic construction provides an alternative for faster, more accurate, and safer installation processes.

The unpredictable nature of typical construction sites and the need to minimize disruptions to surrounding areas require an adaptable and compact robotic system. Cable-Driven Parallel Robots (CDPRs) [7–9] are a type of parallel mechanism where several flexible cables suspend the end-effector. As depicted in Figure 1, CDPRs offer a compact, small-footprint, portable, and easily reconfigurable design, making them ideal for overclad panel installation in densely populated areas with minimal disruption to surroundings. Although the effectiveness of CDPRs at reducing installation time, errors, and costs has been demonstrated with robotic curtain wall installation [10], to the best of our knowledge, this is the first paper on the theoretical optimization of CDPR's size that broadens

their applicability in construction within the constraints of crowded urban environments.

While CDPRs present advantages for panel installation, they face specific challenges and limitations. Unlike traditional rigid-link parallel robots, CDPRs uniquely face the challenge of having cables that can only be driven by positive tension. This characteristic has spurred extensive research in design [11], analysis [12], control [13], and path planning [14]. One particular challenge for automated overclad panel installation is workspace coverage. Ideally, the height and width of the CDPR frame should not exceed the facade dimensions, especially for densely populated areas as pictured in Figure 1. The frame size constraints, coupled with cable force limitations, result in the system being unable to bring the panel to the building corners. This simulation study investigates all possible CDPR designs to determine how much facade coverage the wrench-feasible workspace can achieve. The different models were defined based on their cable configurations. For the most promising models, a frame extension analysis was conducted for both planar and special CDPRs to identify strategies for maximizing coverage.

In the following sections, we begin by reviewing panelized envelope retrofits and CDPRs in construction (Section 2). Next, we discuss the details of CDPRs that can be used for overclad panel installation (Section 3) and wrench-feasible workspace (Section 4). Finally, Section 5 concludes the paper and outlines our future work.

## 2 Related Work

In this section, we will first talk about the background associated with panelized envelope retrofits, then we will review relevant research on CDPRs in construction.

### 2.1 Panelized envelope retrofits

With the growing focus on energy efficiency and sustainability, panelized envelope retrofits [5] have emerged as an essential solution to improve the energy efficiency of older buildings. This retrofit practice uses prefabricated panels for overclad installation over the existing exterior walls and roof. Panelized envelope systems are designed to provide a more efficient and controlled construction process, as the panels are produced under controlled conditions, reducing the potential for on-site errors and improving construction speed. In addition, this method minimizes disruptions to occupants since the overclad panels can be installed with building occupants in place [15].

Traditional approaches for panel installation in multi-story buildings, such as scaffolding, suspended platforms, forklift telehandlers, and stationary or mobile cranes, come with significant drawbacks. They often prove costly, time-consuming, prone to inaccuracies, and require a large

footprint for equipment. For example, scaffolding and suspended platforms, while worker-friendly, are slow and subject to human error, restricting panel size to what can be manually carried. Cranes offer an alternative for large panels, reducing installation time compared to manual methods. However, they remain expensive and relatively slow, with each precast concrete panel taking 15 to 60 minutes to install [16]. Additionally, their large footprint poses challenges in densely populated areas. While addressing a different application, Iturralde *et al.* [10] investigated the work time of using CDPR to install a curtain wall module, reducing installation by 0.51 hours with promising accuracy and repeatability. This achievement holds significant potential to reduce labor costs and increase construction efficiency. With the potential to significantly improve installation speed, reduce costs, and enhance safety, CDPRs are attracting attention for panel installation.

### 2.2 CDPR in Construction

Recently, CDPRs have been explored in various applications and fields [10, 17–24]. Due to their desirable characteristics, such as scalability, reconfigurability, compact design, and high payload-to-weight ratio, they are widely investigated in construction applications such as bricklaying [19–21], 3D printing [22], and solar power plant assembly [23]. For building envelope applications, in particular, Izzard *et al.* [24] explored the use of a CDPR for inspecting building facades. However, the robot was not designed for tight tolerances or heavy payload required for retrofits. In addition, Iturralde *et al.* [10] designed and implemented a CDPR for modular curtain wall installation in real-world application. They investigated whether CDPR could install curtain wall modules with sufficient accuracy and shorten manual installation time. To our knowledge, no prior research has explored the application of CDPRs for automated overclad panel envelope retrofits.

## 3 CDPR for Panelized Envelopes

In this section, we will discuss the specific requirements for CDPR panel installation. We will then analyze various methods to achieve these requirements.

### 3.1 Panelized Envelopes Requirements

Three main requirements are essential for a successful robotic overclad panel envelope retrofit system. Firstly, the CDPR should control the panel's 6 Degrees of Freedom (DOF), including translations and rotations around all three axes. This capability is essential to accommodate non-flat and non-perpendicular walls encountered in real-world residential buildings. Secondly, the CDPR should have enough maneuverability to install panels at any location on the facade (including near corners) without posi-

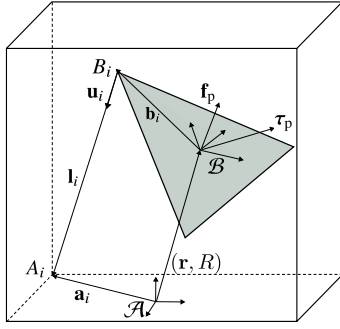


Figure 2. Geometric definitions for a kinematic model of a general CDPR design.

tioning cables between the panel and the facade. Thirdly, the CDPR should have a simple, compact design and a small footprint given that the available installation space may be limited to the building dimensions and the space in front of the building (e.g., sidewalk). Compactness is particularly critical in densely populated urban areas where adjacent buildings or narrow sidewalks impose limitations on the frame size. Simplicity of the frame allows the robot to be installed quickly without the use of a crane.

The CDPR in Figure 1 fulfills the first and third requirements. However, achieving the second requirement requires further exploration. To that end, this paper will study various cable configurations (Section 4.1) and will consider extending the frame size (Section 4.2) in order to improve the facade coverage for panel installation.

### 3.2 CDPR Kinematic Model

In general, a CDPR contains three parts: a fixed frame described in a world coordinate system  $\mathcal{A}$ , a mobile platform (e.g., the panel to be installed) described in a local coordinate system  $\mathcal{B}$ , and  $n$  cables connecting the platform to the frame. The geometric description of the CDPR is shown in Figure 2, which defines the following vectors:

- The constant vectors  $\mathbf{a}_{i \in \{1, \dots, n\}}$  denote the proximal anchor points  $A_i$  in the frame with respect to  $\mathcal{A}$ .
- The constant vectors  $\mathbf{b}_{i \in \{1, \dots, n\}}$ , denote the distal anchor points  $B_i$  in the platform with respect to  $\mathcal{B}$ .
- The platform pose  $(\mathbf{r}, R)$  is defined by the vector  $\mathbf{r}$ , which is the location of the platform's center of mass with respect to  $\mathcal{A}$ , and the rotation matrix  $R \in SO_3$ , which represents the orientation of the mobile platform's frame of reference  $\mathcal{B}$  with respect to  $\mathcal{A}$ .
- The vectors  $\mathbf{l}_{i \in \{1, \dots, n\}}$  represent ideal cables and can be calculated as  $\mathbf{l}_i = \mathbf{a}_i - \mathbf{r} - R\mathbf{b}_i$  with respect to  $\mathcal{A}$ .
- The unit vector along the cable  $\mathbf{u}_i = \mathbf{l}_i / \|\mathbf{l}_i\|_2$ .

- The cable forces  $\mathbf{f}_i = f_i \mathbf{u}_i$ , where  $f_i \geq 0$  are the tensile forces action on each cable  $i \in \{1, \dots, n\}$ .

A simple kinematic model can be constructed by solving the force and torque equilibrium equations as follows:

$$\sum_{i=1}^n \mathbf{f}_i + \mathbf{f}_p = 0 \quad \text{and} \quad \sum_{i=1}^n R\mathbf{b}_i \times \mathbf{f}_i + \boldsymbol{\tau}_p = 0. \quad (1)$$

Here,  $\mathbf{f}_p$  and  $\boldsymbol{\tau}_p$  are the external forces and torques applied to the platform. For our particular application, note that  $\mathbf{f}_p = m\mathbf{g}$  and  $\boldsymbol{\tau}_p = 0$ , where  $m$  is the mass of the overlaid panel. Rewriting Eqn. (1) into matrix form we obtain:

$$\underbrace{\begin{bmatrix} \mathbf{u}_1 & \dots & \mathbf{u}_n \\ R\mathbf{b}_1 \times \mathbf{u}_1 & \dots & R\mathbf{b}_n \times \mathbf{u}_n \end{bmatrix}}_{A^T} \underbrace{\begin{bmatrix} f_1 \\ \vdots \\ f_n \end{bmatrix}}_{\mathbf{f}} + \underbrace{\begin{bmatrix} \mathbf{f}_p \\ \boldsymbol{\tau}_p \end{bmatrix}}_{\mathbf{w}_p} = 0. \quad (2)$$

This can be written in a compact matrix-vector form as  $A^T \mathbf{f} + \mathbf{w}_p = 0$ , where the  $A^T$  is the transpose of the Jacobian matrix and referred to as the *structure matrix*,  $\mathbf{f}$  is the vector of tensile forces, and  $\mathbf{w}_p$  is the total wrench applied.

### 3.3 Wrench-Feasible Workspace

The pose  $(\mathbf{r}, R)$  is called *wrench-feasible* for a given wrench  $\mathbf{w}_p$  if there exists a vector  $\mathbf{f}$  that satisfies:

$$A^T(\mathbf{r}, R)\mathbf{f} + \mathbf{w}_p = 0 \quad \text{s.t.} \quad 0 \leq f_{\min} \leq \mathbf{f} \leq f_{\max} \quad (3)$$

where  $f_{\min}$  and  $f_{\max}$  denote the lower and upper bounds for the feasible force range of the cables. Considering the limited rotation angles required for overlaid panel installation, our analysis assumes that rotation angles are set to zero. Therefore, the wrench-feasible workspace in our study can be defined as:

$$\mathcal{W} = \left\{ \mathbf{r} \mid \text{Eqn. (3) holds with } \mathbf{w}_p = [m\mathbf{g}^T \quad 0]^T \right\}. \quad (4)$$

In general, Eqn. (3) leads to an underdetermined system with either zero or infinitely many solutions. To estimate  $\mathcal{W}$ , a set of poses  $\mathbf{r}$  was selected from a discretized grid, and feasibility was determined using linear programming.

## 4 Analysis of $\mathcal{W}$ for different CDPRs

For ease of visualization and understanding, we will first analyze the wrench-feasible workspace coverage using a planar CDPR. Figure 3 shows the dimensions for a  $1/3$  scaled model of a 3-story residential building currently used at ORNL for building envelope retrofit experiments. The planar CDPR shown in the left plot of Figure 3 corresponds to a 2-translation 1-rotation (2T1R) model with

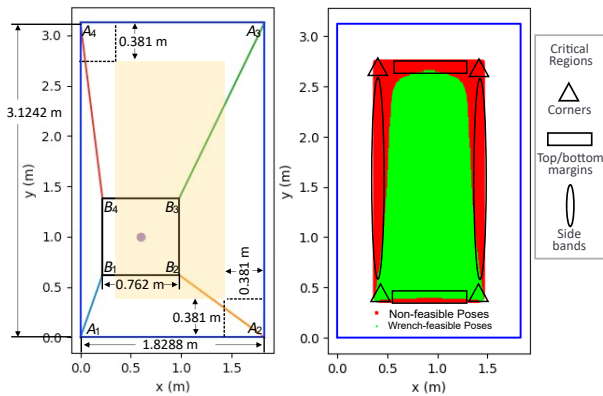


Figure 3. Left: planar CDPR for square panel installation where the frame matches the facade dimensions (blue rectangle). Complete coverage is achieved if the centroid (purple dot) can be moved within the yellow-shaded region. Right:  $\mathcal{W}$  (green area), the red area indicates lack of full coverage.

$n = 4$  cables. The CDPR frame (blue solid line) has the same dimensions as the facade and the square panel (black solid line) can be installed anywhere within the facade. The yellow-shaded region describes the area where the panel's center of mass  $\mathbf{r}$  (purple dot) needs to be maneuvered to fully cover the facade with the panels. Due to inherent limitations imposed by the CDPR's cable arrangement and force restrictions, certain regions of the facade may be difficult to access by most of the configurations. We categorize these regions into three types: corners, top or bottom margins, and lateral bands. The right plot of Figure 3 shows  $\mathcal{W}$  in green color for  $f_{\min} = 132.3$  N,  $f_{\max} = 1200$  N, and  $m = 13.5$  kg. The red colored area shows locations where  $\mathbf{r}$  is required to reach, but there is no feasible solution for Eqn. (3). For this particular CDPR cable arrangement, the top left and right corners, the top and bottom margins, and the side bands of the facade are not reachable, therefore the model in Figure 3 does not provide full facade coverage.

The next sections explore two potential solutions to achieve full facade coverage: adjusting cable configurations and extending the frame size. While this paper ignores cable-to-cable and cable-to-panel collisions, these potential issues can be detected, mitigated, or eliminated in real-world applications through various approaches, such as optimizing cable routing design, applying advanced path planning algorithms, and optimizing anchor positions [7, 25–27]. The following assumptions have been made: (1) all cables are massless, (2) cables don't sag and behave as straight line segments, and (3) the center of mass of the panel coincides with its centroid.

#### 4.1 Analysis of Cable Configurations

The first method to increase the workspace coverage involves exploring alternative cable configurations. For the

Table 1.  $P_{\mathcal{W}}$  for most promising planar CDPRs.

Model#	21	13	15	19	11	12	22	4
$P_{\mathcal{W}}$	1	.88	.83	.83	.79	.78	.76	.73

Table 2. Desired spatial workspace definition.

	$x$	$y$	$z$
Prism start corner (m)	0.381	0.381	0.254
Prism end corner (m)	1.447	2.743	0.9652

planar CDPR with 4 cables, the total number of possible cable configurations is  $4! = 24$ . Figures 4 and 5 illustrate all possible cable configurations and their corresponding wrench-feasible workspaces. Let  $P_{\mathcal{W}}$  denote the wrench-feasible workspace coverage of the CDPR, calculated as the area of  $\mathcal{W}$  divided by the required coverage, i.e., yellow area = green + red areas in Figure 3. Table 1 shows  $P_{\mathcal{W}}$  for the most promising CDPR models. Note that only model 21 achieves  $P_{\mathcal{W}} = 1$ , satisfying the full coverage requirement. By observing all possible cable configurations we concluded that, to maximize  $P_{\mathcal{W}}$ , it is advantageous to connect the proximal anchor to the distal anchor such that the angle between the cable and the closest frame edge is maximized. This is especially useful when the panel needs to reach the corners of the facade. For instance, if the CDPR in model 4 needs to reach an upper corner, the upper cables will form a small angle with respect to the upper frame edge. If the upper cables are close to a horizontal position, their vertical force component will be too small to compensate for gravity. To accommodate for this, the tension on the upper cables needs to increase significantly, saturating the upper limit  $f_{\max}$  and resulting in an infeasible pose. Therefore, in the planar case, the best cable configuration that achieves  $P_{\mathcal{W}} = 1$  is the following:  $\{A_1 \rightarrow B_3, A_2 \rightarrow B_4, A_3 \rightarrow B_1, A_4 \rightarrow B_2\}$ .

Extending our analysis to the spatial case, we consider configurations with 8 cables, 8 distal anchors, and 8 proximal anchors. The parameters employed are identical to those used in the planar case, including a frame depth of 1.219 m and a platform depth of 0.254 m. Note that in real-world panel installation using CDPRs, the dimension of the platform may not be the same as the panel itself. Designing a thicker platform that can carry multiple panels offers a promising approach to reduce the loading time, which can be a significant bottleneck in the installation process. For the spatial analysis, both the CDPR frame and the region where the panel centroid is to be manipulated take the form of rectangular prisms. Table 2 summarizes the dimensions of the desired workspace. Here, the  $x$  and  $y$  axes are the same as in Figure 3, while the  $z$  axis is determined following the right-hand rule. Similar to the previous case, we assumed  $R = I_{3 \times 3}$  for calculating  $\mathcal{W}$ .

The spatial CDPR case yields  $8! = 40,320$  possible cable configurations. However, 63% of them (25,500) lead to

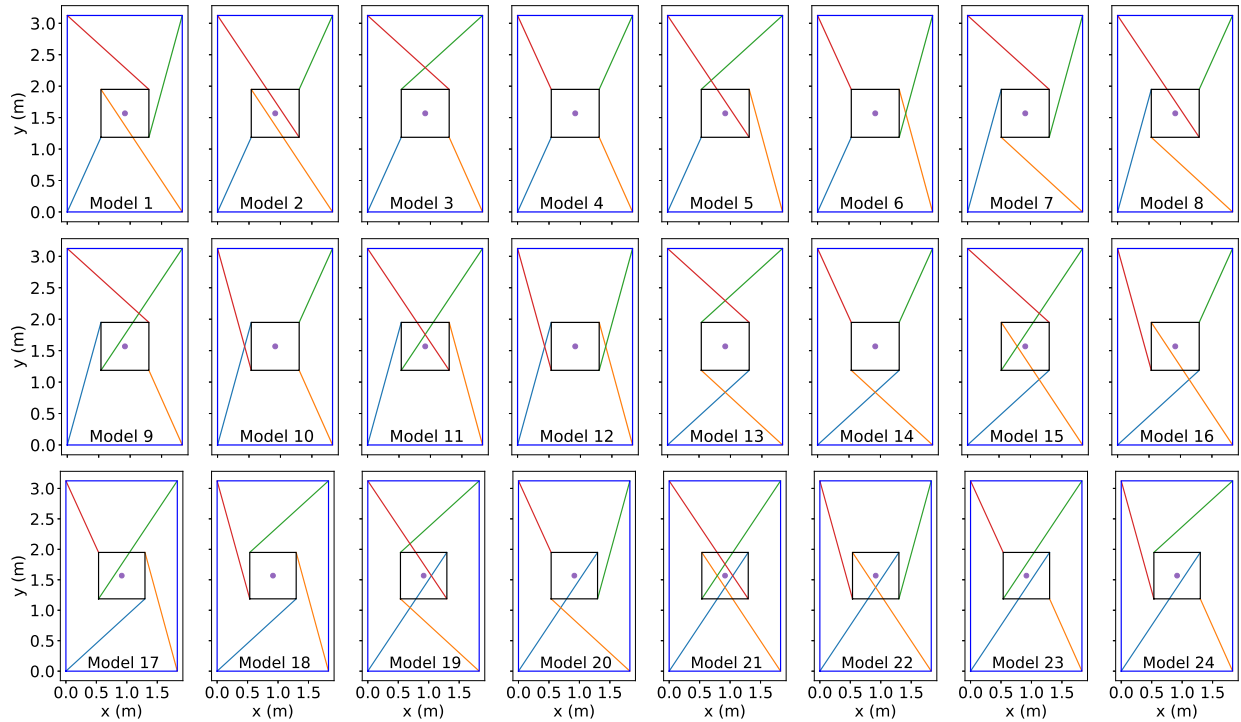


Figure 4. Visualization of all possible cable configurations for planar CDPRs where the frame corners are attached to the panel corners. The model numbers are given for reference.

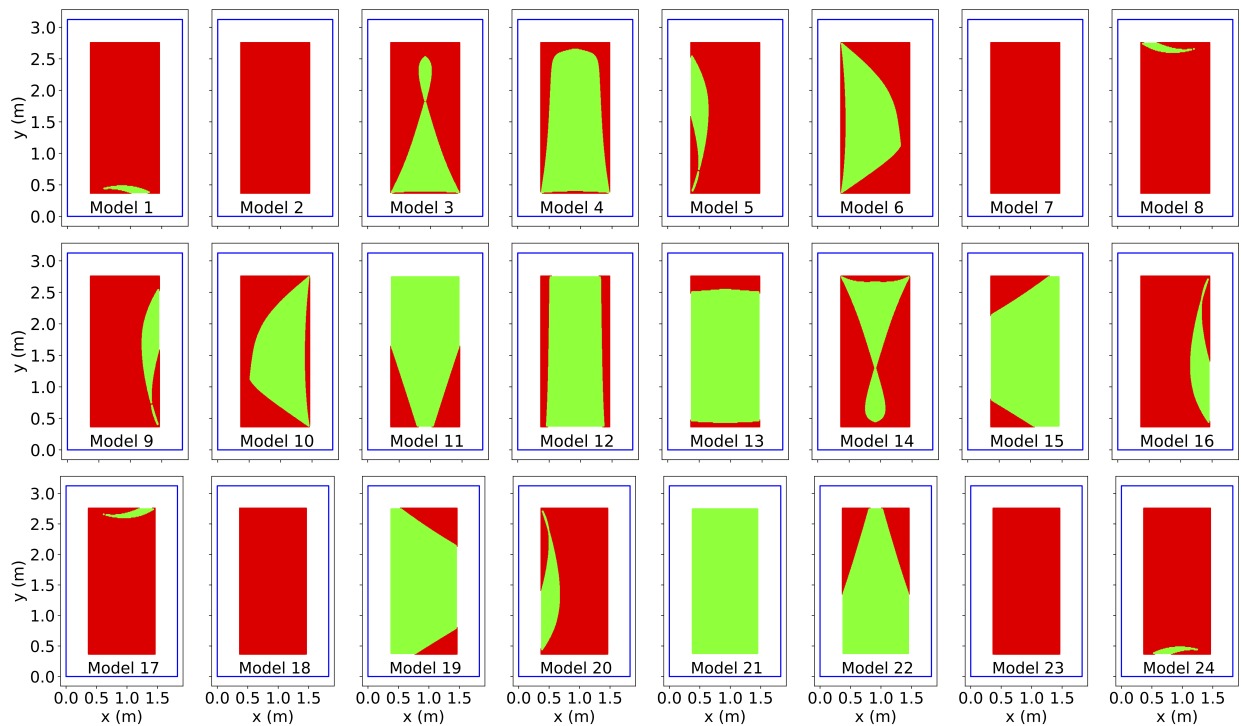


Figure 5. Wrench-feasible workspace  $\mathcal{W}$  (represented in green) for the corresponding planar CDPRs when exploring all possible cable configurations. The red area represents a lack of full facade coverage.

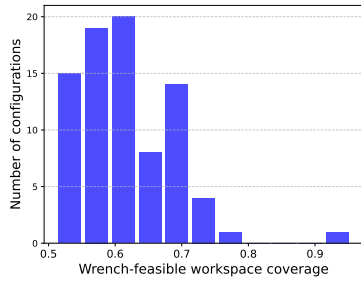


Figure 6. Histogram of  $P_W > 0.5$  for cable-to-panel collision-free spatial CDPR configurations.

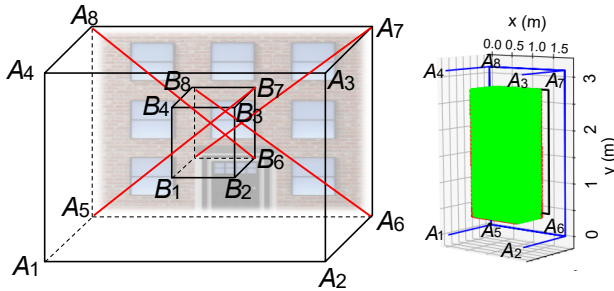


Figure 7. Left: Spatial CDPR model with the largest workspace. We only show cables between the facade and the platform for better visualization. Right:  $\mathcal{W}$ .

cable-to-panel collisions and a substantial portion results in small workspace coverage. Figure 6 shows a histogram depicting the distribution of  $P_W$  for all collision-free configurations with  $P_W > 0.5$ . This analysis reveals that only 82 configurations, out of the original 40,320, achieve a  $P_W > 0.5$ . Due to the retrofitting requirements, positioning cables between the panel and the facade is undesirable. For example, Figure 7 shows the spatial CDPR model with cable configuration  $\{A_1 \rightarrow B_3, A_2 \rightarrow B_4, A_3 \rightarrow B_2, A_4 \rightarrow B_2, A_5 \rightarrow B_7, A_6 \rightarrow B_8, A_7 \rightarrow B_5, A_8 \rightarrow B_6\}$  that achieves  $P_W = 0.95$ . However, the configuration presents an obstruction caused by all the cables between the facade and the platform, hindering panel attachment to the facade. Therefore, we focused our analysis on four specific models that have a large  $P_W$  but do not have cables obstructing the panel installation. Such models are depicted in the first row of Figure 8. From Figures 6 and 8, we can see that achieving 100% coverage of the entire facade is not feasible. Therefore, we should consider an alternative solution: CDPR frame extension.

### 4.2 Frame Extension

Extending the frame size presents another viable solution for increasing the wrench-feasible workspace. Theoretically, the frame can be extended along both width and height, but each approach presents certain limitations. Height extension can only be applied on top of the building and can be impacted by wind loads. Width extension is

applied symmetrically to both the left and right sides and is often constrained by the presence of adjacent buildings. Several factors, including local regulations, infrastructure differences, and community dynamics, can influence the successful implementation of the frame extension. Setting aside local regulations, in densely populated areas, the depth of the frame shouldn't exceed the sidewalk length. For width extension implementation, it is crucial to ensure that the extension does not interfere with adjacent buildings or have any adverse effects on them. Additionally, height extension considerations should be mindful of potential high wind effects. To address safety concerns, a truss-like structure is recommended for supporting the upper cantilevers. Furthermore, it is recommended to shield the frame to prevent pedestrians and workers from harm in the event of cable snapping. Considering the densely populated urban environment depicted in Figure 1, height extension presents a more favorable option due to the limitations inherent in width extension.

To achieve  $P_W = 1$ , different configurations may require different extensions. In the planar case, Model 4 requires height and width extensions, while Model 12 only needs width extension, as illustrated in Figure 9. In the spatial case, Model S1, as shown in Figure 8, fails to reach all corners and leaves a significant gap at the top of the desired workspace. Similar to Model 4 in the planar case, increasing  $P_W$  for Model S1 requires height and width expansions. However, as shown in the third row of Figure 8, achieving full coverage needs substantial extensions on both dimensions, potentially impractical for real-world scenarios. Models S2 and S3 overcome the limitation of not reaching the top of the facade. However, their  $\mathcal{W}$  do not cover the side bands, which demands a width extension to augment  $P_W$ . However, the coverage depicted in plots C(2) and C(3) indicate that even with a 25% width extension,  $P_W$  remains below 1. Model S4 successfully covers the side bands but misses the top and bottom margins. While a height extension can address the top margin coverage, the bottom margin remains inaccessible for this model. When restricted to a single cable configuration, Model S4 is one of the most promising options for maximizing  $P_W$ . Based on our discussion so far, there is currently no single spatial model capable of covering the entire facade area with practical frame extensions. In cases where multiple cable configurations are permitted, a combination of Models S3 and S4 proves effective in covering nearly all areas within the required retrofitting space, except for the four corner areas. The following section will explore potential solutions to address this issue. In addition, depending on the configuration, width or height extensions may not always be beneficial for increasing  $P_W$ . For instance, models S1 and S3 from Figure 8 showcase scenarios where height extension decreases  $P_W$ .

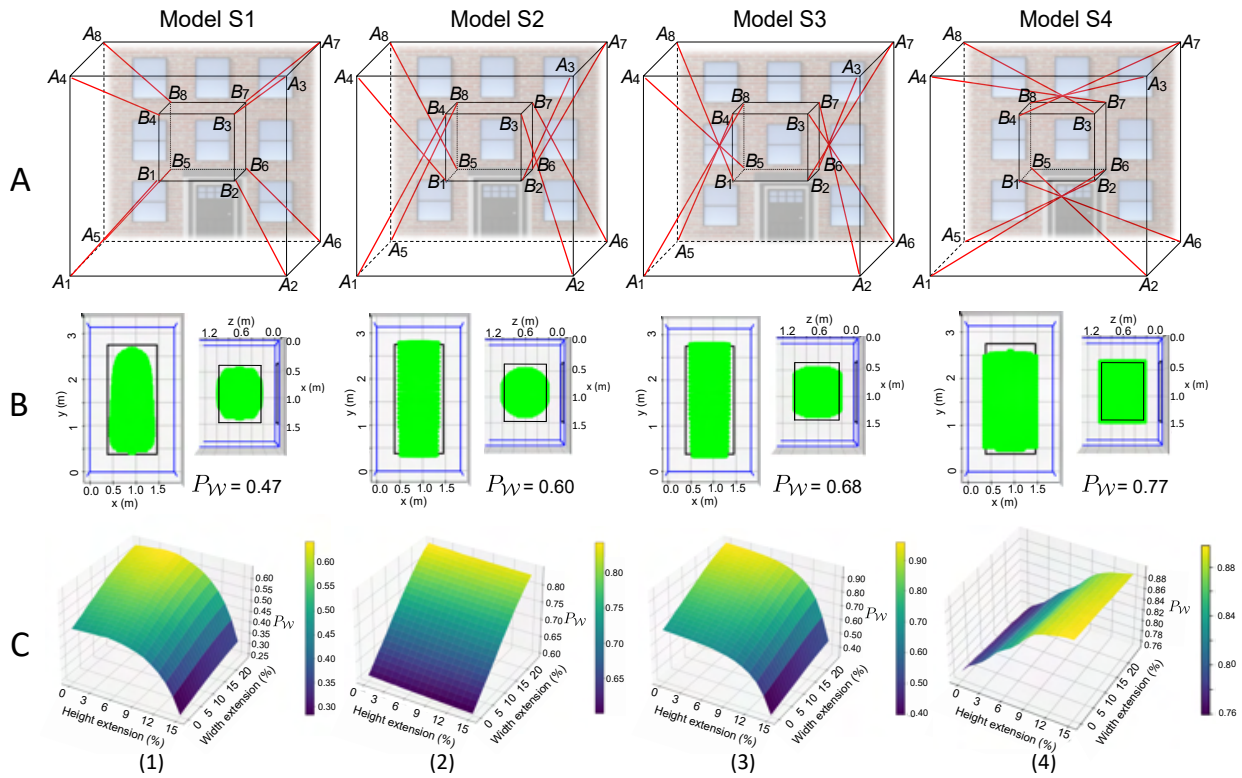


Figure 8. Top: Selected cable configurations. Middle:  $\mathcal{W}$  without frame extension, the black rectangle indicates the panel centroid area needed for a complete retrofit. Bottom:  $P_{\mathcal{W}}$  obtained through frame extension.

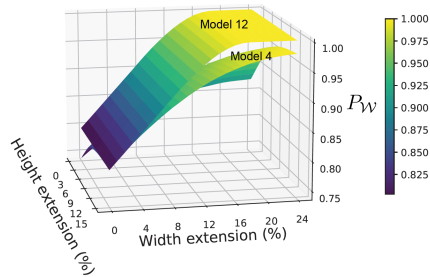


Figure 9. Planar CDRP  $P_{\mathcal{W}}$  comparison for models 4 and 12 with height and width extensions.

## 5 Conclusion and Future Work

This paper studied the use of CDRPs for automated overlaid panel installation. To fulfill envelope retrofit requirements, we explored strategies for maximizing the wrench-feasible workspace. Different cable configurations lead to different wrench-feasible workspace coverage. In general, both width and height extensions improved the coverage for a given configuration. However, if width extension is not feasible, implementing height extension can still improve coverage. This study highlights the importance of considering different cable configurations and frame extension to optimize coverage in different scenarios.

Future research will continue to explore strategies to enhance coverage. Designing reconfigurable anchors of-

fers a potential solution to achieve full coverage. For instance, the combination of Models S3 and S4 can cover nearly all the required retrofitting area, except for the four corners. To address this limitation, one can attach the distal anchor points to a panel carrier instead of directly attaching them to the panel. The panels can be attached off-center on the carrier, with an offset towards the respective corners, thereby compensating for the infeasible space by the original models. Additionally, approaches like optimizing panel and carrier dimensions or designing advanced path planning algorithms by strategically sagging specific cables offer the potential for further increasing workspace coverage. We also intend to expand our research to incorporate a real-world model, aiming to offer a more comprehensive understanding of the entire system. This expansion includes dynamic modeling and control algorithms to evaluate aspects like the system's robustness, autonomy, and applicability to different construction processes, including considerations of economic viability and long-term durability.

## Acknowledgements

This research was supported by the DOE Office of Energy Efficiency and Renewable Energy (EERE), Building Technologies Office, under the guidance of Sven Mumme,

and used resources at the Building Technologies Research and Integration Center (BTRIC), a DOE-EERE User Facility at Oak Ridge National Laboratory.

## References

- [1] U.S. Energy Information Administration. Monthly energy review-november 2023. Technical report, US Energy Information Administration, 2023.
- [2] The American Council for an Energy-Efficient Economy. Energy efficiency impact report. Technical report, 2022.
- [3] Chrissi A Antonopoulos, Cheryn E Metzger, et al. Wall upgrades for residential deep energy retrofits: A literature review. 2019.
- [4] Office of Energy Efficiency & Renewable Energy. Affordable home energy shot. On-line: <https://www.energy.gov/eere/affordable-home-energy-shot#:~:text=Through%20this%20Energy%20Earthshot%2C%20DOE,to%20achieving%20this%20bold%20goal.>, Accessed: 03/14/2024.
- [5] Mikael Salonvaara, Antonio Aldykiewicz Jr, et al. Cost assessment of building envelope retrofits. Technical report, Oak Ridge National Lab.(ORNL), Oak Ridge, TN (United States), 2020.
- [6] Christian Mascheck. Serielles sanieren: So funktioniert der "energiesprong". On-line: <https://cradle-mag.de/artikel/serielles-sanieren-energiesprong.html>, Accessed: 12/15/2023.
- [7] Andreas Pott and Tobias Bruckmann. *Cable-driven parallel robots*. Springer, 2013.
- [8] Zhaokun Zhang, Zhufeng Shao, et al. State-of-the-art on theories and applications of cable-driven parallel robots. *Frontiers of Mechanical Engineering*, 17(3), 2022.
- [9] N. G. Dagalakis, J. S. Albus, et al. Stiffness Study of a Parallel Link Robot Crane for Shipbuilding Applications. *Journal of Offshore Mechanics and Arctic Engineering*, 111(3):183–193, 08 1989. ISSN 0892-7219.
- [10] Kepa Iturralde, Malte Feucht, et al. Cable-driven parallel robot for curtain wall module installation. *Automation in Construction*, 138:104235, 2022.
- [11] Jean-Baptiste Izard, Alexandre Dubor, et al. On the improvements of a cable-driven parallel robot for achieving additive manufacturing for construction. In *Cable-Driven Parallel Robots: Proceedings of the Third International Conference on Cable-Driven Parallel Robots*, pages 353–363. Springer, 2018.
- [12] Zane Zake, Stéphane Caro, et al. Stability analysis of pose-based visual servoing control of cable-driven parallel robots. In *Cable-Driven Parallel Robots: Proceedings of the 4th International Conference on Cable-Driven Parallel Robots 4*, pages 73–84. Springer, 2019.
- [13] João Cavalcanti Santos, Ahmed Chemori, and Marc Gouttefarde. Model predictive control of large-dimension cable-driven parallel robots. In *Cable-Driven Parallel Robots: Proceedings of the 4th International Conference on Cable-Driven Parallel Robots 4*, pages 221–232. Springer, 2019.
- [14] Ricard Bordalba, Josep M Porta, and Lluís Ros. Randomized kinodynamic planning for cable-suspended parallel robots. In *Cable-Driven Parallel Robots: Proceedings of the Third International Conference on Cable-Driven Parallel Robots*, pages 195–206. Springer, 2018.
- [15] Robert P Sroufe, Craig E Stevenson, et al. The building envelope holds the key. *The Power of Existing Buildings: Save Money, Improve Health, and Reduce Environmental Impacts*, pages 85–105, 2019.
- [16] Nolan Hayes and Diana Hun. Expediting pre-cast concrete installation. On-line: [https://lsc-pagepro.mydigitalpublication.com/publication/?i=806162&article\\_id=4666276&view=articleBrowser](https://lsc-pagepro.mydigitalpublication.com/publication/?i=806162&article_id=4666276&view=articleBrowser), Accessed: 12/18/2023.
- [17] Andreas Pott, Hendrick Mütterich, et al. Ipanema: a family of cable-driven parallel robots for industrial applications. *Cable-Driven Parallel Robots*, pages 119–134, 2013.
- [18] Rendong Nan. Five hundred meter aperture spherical radio telescope (fast). *Science in China Series G*, 49(2), 2006.
- [19] Yulong Wu, Hung Hon Cheng, et al. Cu-brick cable-driven robot for automated construction of complex brick structures: From simulation to hardware realisation. In *2018 IEEE International Conference on Simulation, Modeling, and Programming for Autonomous Robots (SIMPAR)*, pages 166–173. IEEE, 2018.
- [20] Ilija Vukorep. Autonomous big-scale additive manufacturing using cable-driven robots. In *Proceedings of the 34th International Symposium on Automation and Robotics in Construction (ISARC)*, pages 254–259, Taipei, Taiwan, July 2017. Tribun EU, s.r.o., Brno. ISBN 978-80-263-1371-7.
- [21] Tobias Bruckmann, Christopher Reichert, et al. Concept studies of automated construction using cable-driven parallel robots. In Clément Gosselin, Philippe Cardou, Tobias Bruckmann, and Andreas Pott, editors, *Cable-Driven Parallel Robots*, pages 364–375, Cham, 2018. Springer International Publishing. ISBN 978-3-319-61431-1.
- [22] Paul Bosscher, Robert L. Williams, et al. Cable-suspended robotic contour crafting system. *Automation in Construction*, 17(1):45–55, 2007. ISSN 0926-5805.
- [23] Andreas Pott, Christian Meyer, and Alexander Verl. Large-scale assembly of solar power plants with parallel cable robots. In *ISR 2010 (41st International Symposium on Robotics) and ROBOTIK 2010 (6th German Conference on Robotics)*, pages 1–6, 2010.
- [24] Jean-Baptiste Izard, Marc Gouttefarde, et al. *Integration of a Parallel Cable-Driven Robot on an Existing Building Façade*, pages 149–164. Springer Berlin Heidelberg, Berlin, Heidelberg, 2013. ISBN 978-3-642-31988-4.
- [25] Vincentius A Handojo, Adlina T Syamlan, et al. Cable driven parallel robot with big interference-free workspace. In *Mechanism and Machine Science: Select Proceedings of Asian MMS 2018*, pages 43–56. Springer, 2020.
- [26] Jeong-Hyeon Bak, Sung Wook Hwang, et al. Collision-free path planning of cable-driven parallel robots in cluttered environments. *Intelligent Service Robotics*, 12:243–253, 2019.
- [27] Martin J-D Otis, Simon Perreault, et al. Determination and management of cable interferences between two 6-dof foot platforms in a cable-driven locomotion interface. *IEEE Transactions on Systems, Man, and Cybernetics-Part A: Systems and Humans*, 39(3):528–544, 2009.